



Simultaneous all-channel OTDM demultiplexing based on complete optical Fourier transformation

Guan, Pengyu; Lillieholm, Mads; Røge, Kasper Meldgaard; Morioka, Toshio; Oxenløwe, Leif Katsuo

Published in:

Proceedings of 2016 21st OptoElectronics and Communications Conference

Publication date:

2016

Document Version

Peer reviewed version

[Link back to DTU Orbit](#)

Citation (APA):

Guan, P., Lillieholm, M., Røge, K. M., Morioka, T., & Oxenløwe, L. K. (2016). Simultaneous all-channel OTDM demultiplexing based on complete optical Fourier transformation. In Proceedings of 2016 21st OptoElectronics and Communications Conference IEEE.

General rights

Copyright and moral rights for the publications made accessible in the public portal are retained by the authors and/or other copyright owners and it is a condition of accessing publications that users recognise and abide by the legal requirements associated with these rights.

- Users may download and print one copy of any publication from the public portal for the purpose of private study or research.
- You may not further distribute the material or use it for any profit-making activity or commercial gain
- You may freely distribute the URL identifying the publication in the public portal

If you believe that this document breaches copyright please contact us providing details, and we will remove access to the work immediately and investigate your claim.

Simultaneous All-channel OTDM Demultiplexing Based on Complete Optical Fourier Transformation

Pengyu Guan, Mads Lillieholm, Kasper Meldgaard Røge, Toshio Morioka, Leif Katsuo Oxenløwe
DTU Fotonik, Technical University of Denmark, Ørstedss Plads, 343, Kgs. Lyngby, 2800, Denmark
pengu@fotonik.dtu.dk

Abstract: We demonstrate simultaneous OTDM demultiplexing of all 16-channels for 160-Gbit/s DPSK and 320-Gbit/s DQPSK signals based on complete OFT. Furthermore, numerical simulations show promising results for extending the proposed technique to spectrally efficient Nyquist-OTDM.

Keywords: Optical signal processing; Optical demultiplexing; Optical Fourier transformation.

I. INTRODUCTION

Optical Time-Division Multiplexing (OTDM) is the time-interleaving of optical data signals generated from lower rate pulse trains at identical wavelengths. OTDM enables us to realize future ultrahigh-capacity optical networks with an increased bit rate per wavelength channel and decreased channel numbers. Thus, the number of components as well as the system complexity and power consumption, are reduced. Single-channel 10.2-Tb/s and 1.92-Tb/s OTDM transmissions have already been demonstrated with advanced modulation formats [1-2]. One of the key enabling technologies for such an ultrahigh-speed OTDM system is an optical demultiplexer, which can be realized by an optical temporal switch such as a nonlinear optical loop mirror [3], a Kerr switch [4] or a symmetric Mach-Zehnder device [5]. However, using these schemes to fully demultiplex an OTDM signal requires one optical temporal switch per channel. Therefore, the complexity of an OTDM receiver essentially scales with the number of OTDM channels. To overcome this problem, a new approach for OTDM demultiplexing based on a “partial” optical Fourier transformation (OFT) has been proposed [6]. Such a “partial” OFT allows several OTDM channels to be demultiplexed simultaneously. However, all-channel OTDM demultiplexing is still very challenging due to the inter-channel crosstalk produced by the “partial” OFT process [7].

Previously we have proposed a “complete” OFT scheme for all-channel serial-to-parallel conversion [8]. In this paper, we present the experimental demonstration of 160-Gbit/s DPSK and 320-Gbit/s DQPSK all-channel simultaneous OTDM demultiplexing using a complete OFT. Full system characterizations with bit error rate (BER) measurements are performed. For 160-Gbit/s OTDM-DPSK demultiplexing, error-free performance was achieved for all OTDM channels with an average power penalty of only 1.2 dB at BER = 10^{-9} . For 320-Gbit/s DQPSK signal, a BER performance below the FEC limit (2×10^{-3}) is achieved for all demultiplexed channels. In addition, detailed Monte Carlo BER simulations predict that the proposed scheme will also perform well for Nyquist-OTDM demultiplexing.

II. PRINCIPLE AND EXPERIMENTAL DEMONSTRATION

The OFT is based on the principle of a “time-lens”, originating in the space-time duality of light. It can transfer the temporal profile of an optical signal into the frequency domain or vice-versa. The traditional OFT for OTDM demultiplexing consists of a dispersive medium with $D = \beta_2 L$ (β_2 is the second order dispersion and L is the length), followed by a quadratic phase-modulation stage ($\delta\phi = Kt^2/2$) with chirp rate K , satisfying the condition $K = 1/D$, and has been used in many demonstrations [6-7]. However, it is not suitable for all-channel simultaneous OTDM demultiplexing. Since the dispersive elements before the phase modulation stage will generally broaden the input waveform causing temporal clipping and hence spectral broadening and power loss of the edge channels after OFT, large inter-channel crosstalk and OSNR degradation occurs. To overcome this problem, we propose to use a new time-lens based complete OFT, which has already been used in demonstrations for WDM to Nyquist-OTDM conversion [9]

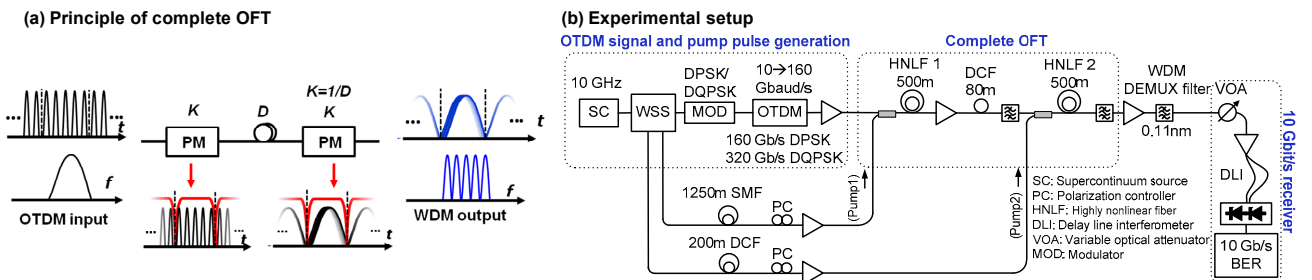


Fig. 1. (a) Schematic diagrams of a time-lens based complete OFT. (b) Experimental setup for 160 Gbit/s DPSK and 320 Gbit/s DQPSK all-channel OTDM demultiplexing

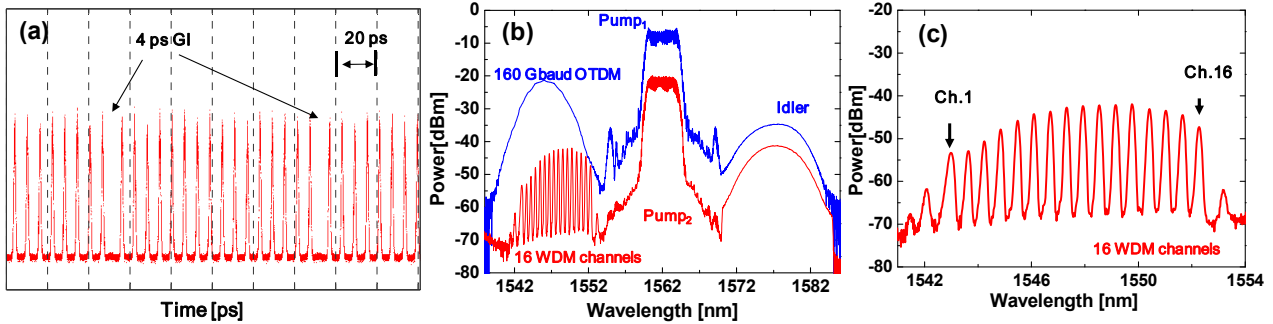


Fig. 2. Results of OTDM to WDM conversion. (a) 160 Gbaud OTDM signal waveform, (b) optical spectrum after the first (blue curve) and second (red curve) FWM process, (c) spectrum of the 16 obtained WDM channels.

and for OFDM to Nyquist-WDM conversion [10]. The schematic diagram of this OFT is shown in Fig. 1(a), where two quadratic phase-modulation stages with chirp rate K , separated by a medium with accumulated dispersion D , which satisfies the condition $K = 1/D$ (a K - D - K configuration). With this configuration, all input OTDM channels are pre-chirped by the first time-lens. The chirped signals propagating in the dispersive medium will not only experience waveform broadening, but also become aligned (focused) to the center of the second phase-modulation stages. This configuration thus confines the waveform to the time-lens apertures, making it suitable for a simultaneous, all-channel OTDM to WDM conversion (a “complete” OFT). The converted WDM signal can be simply demultiplexed by a passive WDM demultiplexer. The chirp rate K determines the scaling factor between the time- and frequency-domains according to $\Delta t = 2\pi\Delta f/K$.

The experimental setup is shown in Fig. 1(b). A supercontinuum signal is generated by a 10-GHz mode-locked laser and a 400-m dispersion-flattened highly non-linear fiber (DF-HNLF). The broadened spectrum is Gaussian-filtered at 1546 nm by a programmable wavelength selective switch (WSS). The obtained 1 ps pulses train is DPSK or DQPSK modulated using an IQ modulator. The 10-Gbaud modulated signal is then OTDM-multiplexed to 160 Gbaud, resulting in a 160-Gbit/s DPSK-OTDM signal or a 320-Gbit/s DQPSK-OTDM signal. Fig. 3(a) shows the obtained 160-Gbaud OTDM signal waveform with a tributary spacing of 6 ps. A 4 ps guard interval is inserted after every 16 tributaries to allow for the transition between consecutive quadratic phase-modulation windows. A complete OFT is used for the all-channel OTDM-to-WDM conversion. The quadratic phase modulation is based on a four-wave mixing (FWM) in a highly non-linear fiber (HNLF) using linearly chirped (quadratic phase) rectangular pump pulses at 10 GHz. Both pump pulses and the data signal are obtained from the same broadened spectrum using a WSS. To obtain linearly chirped pumps, the filtered pump1 and pump2 are subsequently propagated in a 1250 m SMF and 200 m dispersion compensating fiber (DCF), respectively. The chirp rate $K = 0.078 \text{ ps}^{-2}$ is set for conversion of the 6 ps temporal spacing to a 75-GHz (0.6 nm) frequency grid. The first FWM output is shown in Fig. 2(b). After extraction with a 15 nm optical bandpass filter (OBPF), the idler is dispersed in 80 m DCF corresponding to dispersion D , and subsequently combined with pump2 and coupled into HNLF₂ for the second FWM process. The resulting spectrum is also shown in Fig. 3(b). The generated idler is the 16-channel WDM signal converted from the 160-Gbaud OTDM signal. Fig. 3(c) shows a zoom-in of the generated idler, where 16 WDM channels with 75 GHz (0.6 nm) spacing can be observed. High extinction ratios of 25 dB and 17 dB, are observed for the center and left edge channels respectively. The skew between the channels is caused by the limited FWM bandwidth of the used HNLFs. This indicates insignificant spectral channel overlap, resulting in a crosstalk-less all-channel OTDM demultiplexing. In the receiver, a 14-GHz (0.11 nm) Gaussian filter is used to demultiplex each WDM channel. Finally, the BER of each demultiplexed DPSK or DQPSK channel is measured in a pre-amplified receiver including a delay-line interferometer (DLI) and a balanced photo-detector.

The BER measurements for all 16 demultiplexed 10-Gbit/s DPSK channels are shown in Fig. 3(a), where error free performance ($\text{BER} < 10^{-9}$) is achieved for all DPSK-OTDM channels with an average receiver sensitivity of -40.5 dBm. The average power penalty at $\text{BER} = 10^{-9}$ is only 1.2 dB compared to the 10 Gbit/s DPSK baseline. The BER measurements for 320-Gbit/s DQPSK-OTDM demultiplexing are shown in Fig. 3(b) for selected DQPSK channels. As

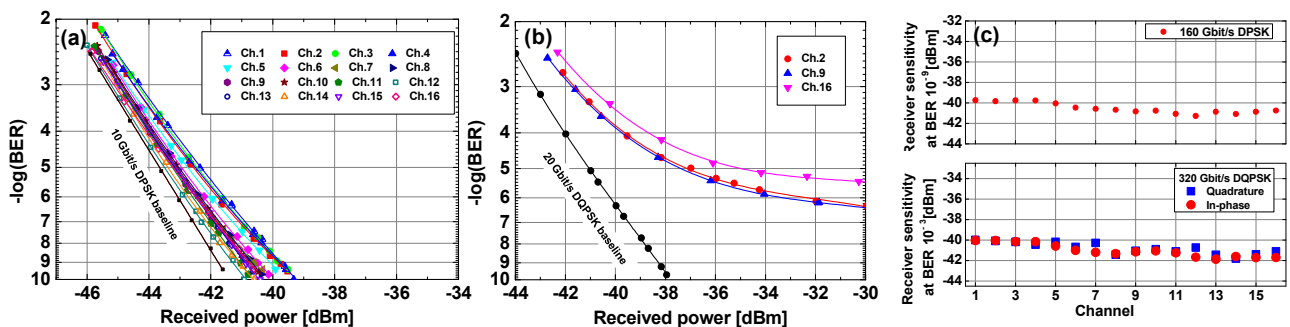


Fig. 3. Experimental results. (a) BER performance of all 16 demultiplexed 10-Gbit/s DPSK channels, (b) BER performance for selected demultiplexed DQPSK channels, (c) receiver sensitivities at $\text{BER} = 10^{-9}$ of all demultiplexed DPSK channels, and receiver sensitivities at $\text{BER} = 10^{-3}$ of all DQPSK channels.

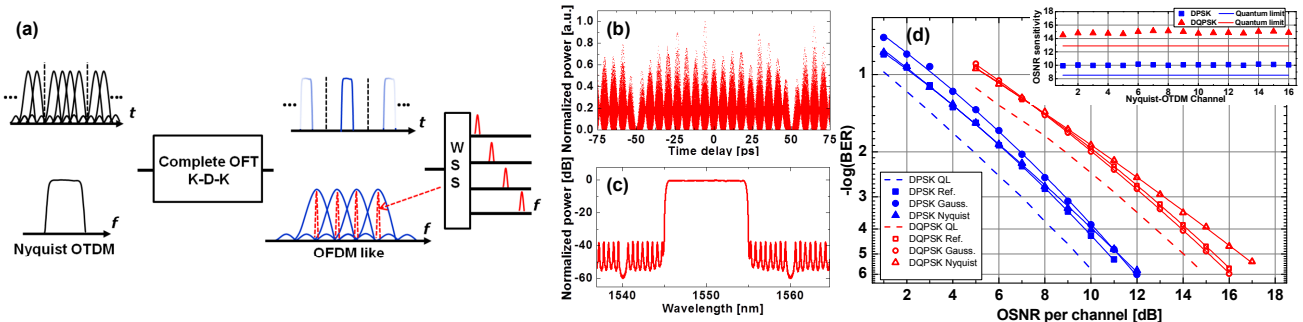


Fig. 4. Numerical simulations for all-channel Nyquist-OTDM demultiplexing, (a) schematic diagrams, (b) waveform of 160 Gbaud Nyquist-OTDM signal, (c) OFT output spectrum, (d) BER performance for 160 Gbit/s DPSK and 320 Gbit/s DQPSK signals. The inset shows the corresponding OSNR sensitivities at $\text{BER} = 10^{-4}$ of all demultiplexed 10 Gbit/s DPSK and 20 Gbit/s DQPSK channels.

The DQPSK signals have a higher OSNR requirement and a lower phase noise tolerance than DPSK signals at the same baud rate, there are error floors around 10^{-5} and 10^{-6} due to the nonlinear phase noise and OSNR degradation introduced by the FWM processes. Fig. 3(c) shows the receiver sensitivities at $\text{BER} = 10^{-9}$ of all demultiplexed DPSK-OTDM channels, as well as the receiver sensitivities at $\text{BER} = 10^{-3}$ of all demultiplexed DQPSK-OTDM channels. The DQPSK demonstration confirms the fact that the proposed scheme can be applied to complex modulation formats.

III. NUMERICAL SIMULATIONS FOR NYQUIST-OTDM DEMULTIPLEXING

Nyquist-OTDM signals take advantage of orthogonality in the time domain, which enables high bit rates with high spectral efficiency [11]. We performed Monte Carlo simulations to investigate the proposed scheme for all-channel Nyquist-OTDM demultiplexing. Fig. 4(a) shows the schematic diagrams of the simulations. A 160-Gbaud Nyquist-OTDM signal with 5.9 ps (1/170 GHz) channel spacing is converted into 16 sinc-shaped multi-carriers at different frequencies simultaneously using a complete OFT. As the tributaries of the Nyquist-OTDM are all overlapping seamlessly, it is essential to insert a short guard-interval (5.9 ps) after every 16 tributaries for OFT operation. The waveform of the 160-Gbaud Nyquist-OTDM signal is shown in Fig. 4(b). The chirp rate, $K = 0.078 \text{ ps}^{-2}$, is set for conversion of the 5.9 ps OTDM spacing to a 73 GHz (0.59 nm) frequency grid. Fig. 4(c) shows the OFT output spectrum. A bank of 24-GHz passive Gaussian filters with 73 GHz spacing is used to extract all converted channels at the crosstalk-less positions. The Nyquist-OTDM channels are independently data-modulated with random and uniformly distributed bits using either DPSK or DQPSK. The demultiplexed channels are detected using an ASE limited receiver consisting of a 10-GHz DLI and a BPD (no detector noise). To estimate the BER, iterations of 1024 symbols are repeated until at least 100 errors are observed. Each BER value is obtained by averaging over 5 simulations. The results are shown in Fig. 5 as the BER vs OSNR per subcarrier for both 160-Gbaud Nyquist-OTDM (sinc shaped) and normal OTDM (Gaussian shaped) signals. The inset shows the corresponding OSNR sensitivities at $\text{BER} = 10^{-4}$ for all demultiplexed 10-Gbit/s DPSK and 20-Gbit/s DQPSK Nyquist-OTDM channels. As a reference, we calculate the BER performance in the absence of neighboring OTDM channels (denoted as Ref) after the OFT. The quantum limit for the reference (matched optical filter and no electrical filtering) is also shown (denoted as QL). The simulation results indicate that the proposed scheme enables all-channel Nyquist-OTDM demultiplexing with a $\text{BER} < 10^{-5}$ for both DPSK and DQPSK signals. For DPSK, the OSNR penalty due to the crosstalk from neighboring Nyquist-OTDM channel is negligible relative to the reference and normal OTDM (down to $\text{BER} \sim 10^{-5}$). For DQPSK, the OSNR penalty increases to $\sim 1 \text{ dB}$ at $\text{BER} = 10^{-5}$, due to the lower crosstalk tolerance for DQPSK signals.

IV. CONCLUSIONS

We have demonstrated 160-Gbit/s DPSK and 320-Gbit/s DQPSK simultaneous all-channel OTDM demultiplexing using a complete OFT. All-channel error-free performance was achieved for 160 Gbit/s DPSK signal. For a 320-Gbit/s DQPSK signal, a BER performance below the FEC limit (2×10^{-3}) is achieved for all demultiplexed channels. Furthermore, Monte Carlo simulations indicate that the proposed scheme can also be advantageously used for simultaneous all-channel Nyquist-OTDM demultiplexing.

ACKNOWLEDGMENT

OFS Denmark Aps, Danish Research Council: FTP project TOR (ref. no. 12-127224), FTP project LENS-COM (ref. DFF-5054-00184) and the DFF Sap. Aude Adv. Grant NANO-SPECs (DFF-4005-00558B).

REFERENCES

- [1] T. Richter et al., in Proc. OFC 2011, PDPA9, (2011).
- [2] D. O. Otuya et al., Opt. Express, 21(19), 22808 (2013).
- [3] N. J. Doran et al., Opt. Lett., vol. 13, 56–58, (1988)
- [4] T. Morioka et al., Electron. Lett., 23 (9), 453-454, (1987).
- [5] T. Hirooka et al., IEEE PTL., 21(20), 1574-1576, (2009).
- [6] H. C. H. Mulvad et al., Proc. OFC 2011, OThN2, (2011).
- [7] K. G. Petrillo et al., Proc. CISS, 1-6, (2013).
- [8] P. Guan et al., Proc. OFC 2016, W3D.2, (2016).
- [9] P. Guan et al., Proc. ECOC, We.2.5.5, (2014).
- [10] P. Guan et al., IEEE JLT, 34(2) 626-632 (2015).
- [11] M. Nakazawa et al., Opt. Express, 20(2), 1129,(2012).